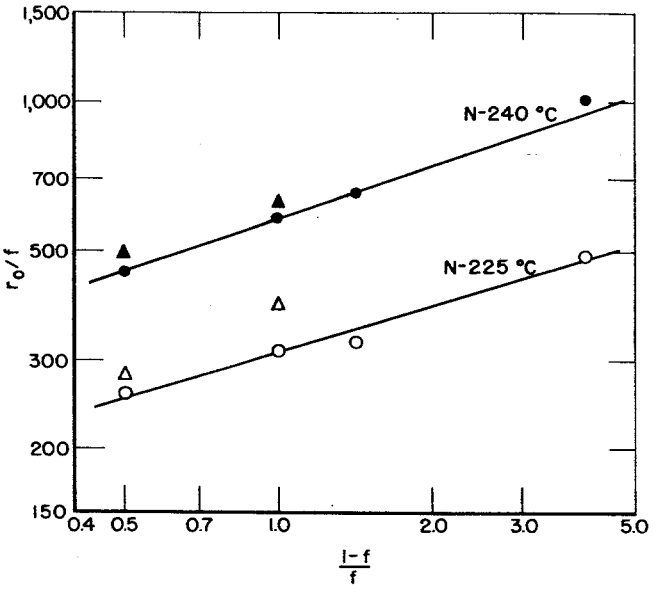


FIGURE 7.—Plots of Equation (10) for Reduced and Nitrided Catalysts. △ and ▲ Represent Reduced Catalysts at 240° and 255° C, Respectively; ○ and ● Represent Nitrided Catalysts at 225° and 240° C, Respectively.

process is inhibited by products of the reaction, possibly carbon dioxide but more likely water vapor. As the activity of iron catalysts is not significantly impaired by submersing the catalyst in synthesis oils, the inhibition of rate observed in the present experiments can hardly be attributed to hydrocarbon.

Uchida and coworkers (*64*) investigated the kinetics of the Fischer-Tropsch synthesis on iron catalysts with $1H_2+1CO$ gas at 24 atmospheres, tested several rate equations, and obtained reasonable agreement for three of these equations. However, the equations considered satisfactory by Uchida and most other rate equations of Hougen and Watson type (*30*) cannot account for the first-order dependence of rate on operating pressure and at the same time provide the proper decrease in rate with increasing concentration of products.

## EFFECT OF VARIABLES OF OPERATION ON SELECTIVITY

Selectivity data are reported for experiments with nitrided iron catalysts at 225° and 240° C and 21.4 atmospheres with feed gases varying from $2H_2+1CO$ to $0.25H_2+1CO$; rate data for these experiments were reported in previous sections (*32*). As data at 225° and 240° C showed the same trends and usually only minor quantitative differences, only experimental points for tests at 225° C are shown in several of the figures.

Figure 11 presents plots of the relative usage of hydrogen, moles of $H_2$ consumed per mole of $H_2+CO$ consumed, as a function of fraction of $H_2+CO$ reacted, $x$. These plots are of the form $m_{H_2}/x$ as a function of $x$, where $m_{H_2}$ is given as moles $H_2$ consumed per mole of $H_2+CO$ feed. In these plots if $x=1$, the relative usage of hydrogen must equal the feed ratio; these points are designated by solid symbols. For $0.25H_2+1CO$ gas a point is also shown for the maximum conversion possible with a usage ratio of $H_2$ to CO of 0.5.

The general trend of the differential selectivity, $dm_{H_2}/dx$, can be constructed readily from the integral curves of figure 11 using the relationship $dm_{H_2}/dx=m_{H_2}/x$ at $x=0$ and at $d^2(m_{H_2}/x)/dx^2=0$.

The relative usage of hydrogen, $m_{H_2}/x$, decreases with decreasing hydrogen content of the feed. With increasing conversion $m_{H_2}/x$ decreases, passes through a minimum (not clearly defined in a few of the present plots), and then increases. Extrapolation to solid points at $x=1$ seems reasonable. With $0.25H_2+1CO$ feed and at conversions greater than about 0.4 for tests at 225° C or greater than 0.5 for tests at 240° C, the relative usage of hydrogen is less than 0.33 which is the lower limit for the production of aliphatic hydrocarbons. Reactions producing carbon, in addition to synthesis, can explain these results.

Similar plots of $CO_2$ production, moles $CO_2$ produced per mole of $H_2+CO$ consumed, $m_{CO_2}/x$, as a function of conversion $x$ increases with increasing values of $x$, passes through a maximum in the range 0.5 to 0.6, and then decreases. The production of $CO_2$ increased with increasing content of carbon monoxide in the feed gas; for example, the maximums for the values of $m_{CO_2}/x$ were 0.20 for $2H_2+1CO$, 0.237 for $1H_2+1CO$, 0.28 for $0.7H_2+1CO$, and 0.325 for $0.25H_2+1CO$. The maximums occur at about the same conversion as the minimums in the curves of figure 11. For all feed compositions except $0.25H_2+1CO$ these maximums should also be expected, because the total

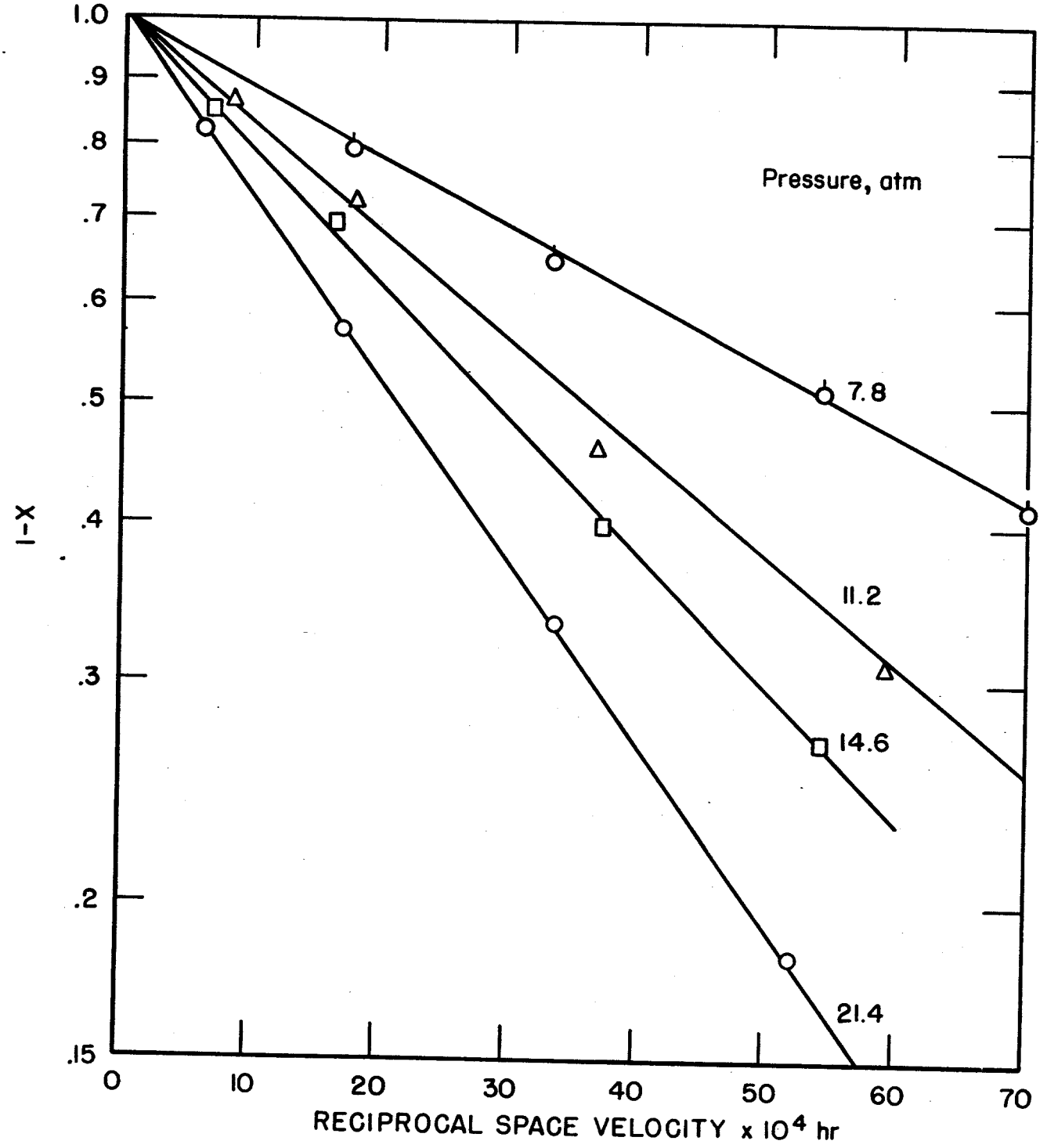


FIGURE 8.—Plots of First-Order Empirical Equation for Nitrided Catalyst D3001 at 240° C With $1H_2+1CO$ gas.

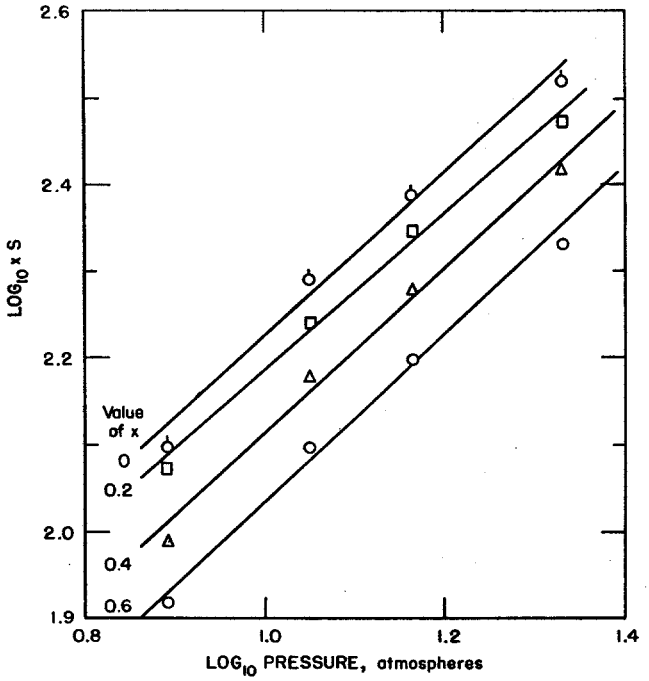


FIGURE 9.—Logarithmic Plots of $(xS)_x$ Against Operating Pressure for Tests With $1H_2+1CO$ at 240° C.

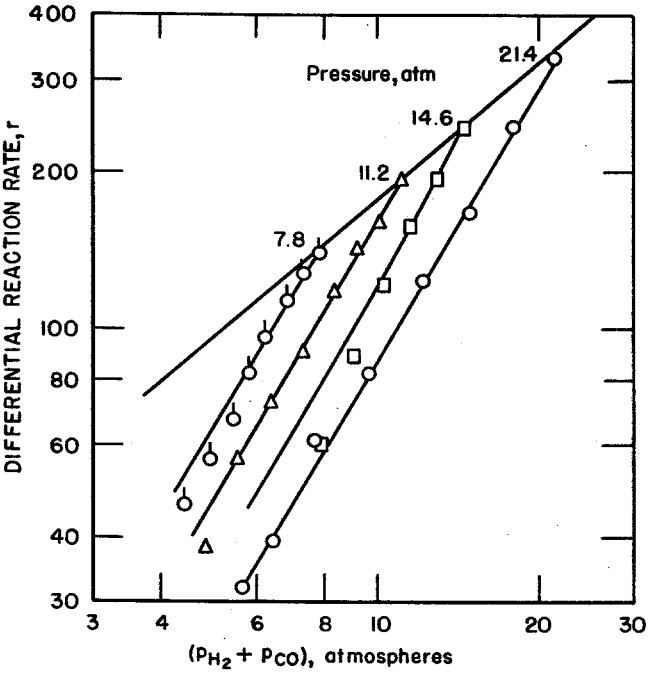


FIGURE 10.—Logarithmic Plots of Differential Reaction Rate $r$ as a Function of Partial Pressure of $H_2+CO$ for Tests With $1H_2+1CO$ at 240° C.

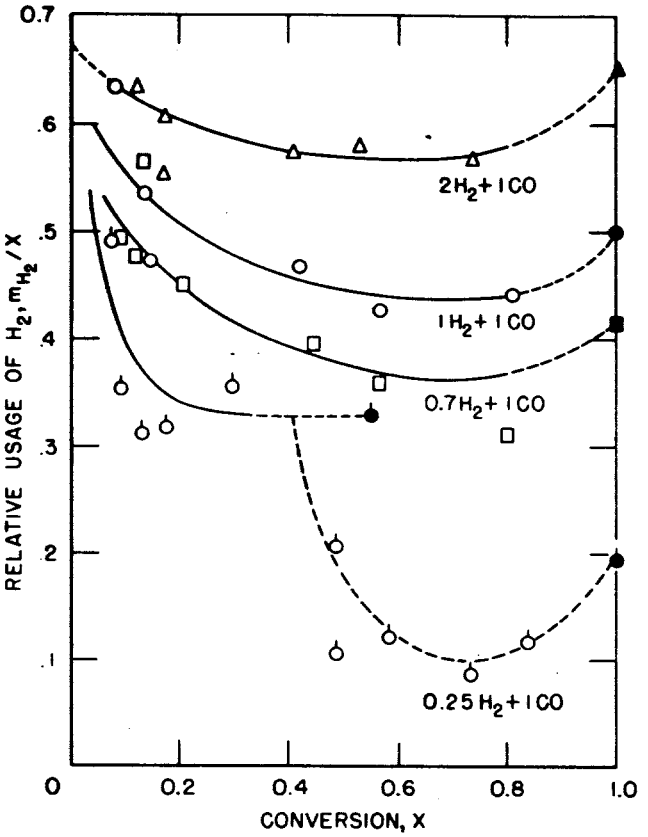


FIGURE 11.—Relative Usage of Hydrogen as a Function of Conversion for Nitrided Catalyst D3001 at 21.4 Atmospheres and 225° C.

consumption of the gas according to equation (1) demands lower final values than the maximum. With $0.25H_2+1CO$ gas at conversions greater than 0.40 at 225° C and 0.5 at 240° C, the process is probably complicated by carbon-forming reactions of the type (1) $2CO \rightarrow C+CO_2$ and (2) $3Fe+4CO \rightarrow Fe_3O_4+4C$. Apparently both reactions occur with reaction (2) increasing in magnitude with increasing conversion; for example, two anomalous values of $m_{CO_2}/x=0.35$ are observed at about $x=0.6$ followed by values decreasing to as low as 0.16 at $x=0.89$.

Methane production (moles $CH_4$ produced per mole of $H_2+CO$ consumed, $m_{CH_4}/x$) in figure 12 is shown to increase with increasing hydrogen content of the feed. All of the curves decrease, pass through a minimum, and then increase as the conversion is increased. Points for $1H_2+1CO$ and $0.7H_2+1CO$ feeds overlap and are represented by a single curve.

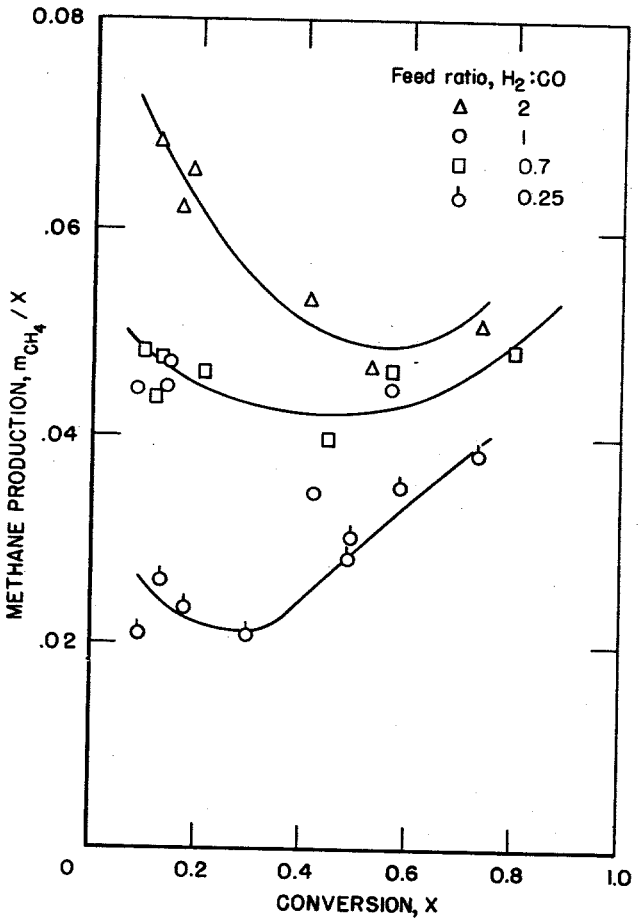


FIGURE 12.—Methane Production as a Function of Conversion for Nitrided Catalyst D3001 at 21.4 Atmospheres and 225° C.

The initial decrease in methane production cannot be explained by variations of the ratio of $H_2$ to CO as the gas is converted, because this ratio increases with conversion for $2H_2+1CO$, $1H_2+1CO$, and $0.7H_2+1CO$ feed gases. Methane formation varies inversely with the concentrations of water vapor and carbon dioxide in this initial portion. However, the increasing ratio of $H_2$ to CO with conversion may eventually produce the minimum and the increasing portion of the curves.

With $0.25H_2+1CO$ feed the minimum and subsequent increase is difficult to explain. Above conversions of 0.65 at 240° C and 0.49 at 225° C the moles of both $H_2$ and $CH_4$ per mole of feed increased. This range includes conversions at which anomalous results were found for the relative usage of hydrogen and production of $CO_2$. Reactions involving dehydrogenation and cracking of molecules adsorbed in pores of the catalyst could provide an explanation of these observations.

The variation of unsaturation in the $C_2$ and $C_3$ fractions as a function of feed composition and conversion is presented in figure 13. As the concentrations of these hydrocarbons in the exit gas were less than 2.5 percent for even the highest conversions, the data proved erratic when calculated in the same way as methane formation; however, reasonable trends were obtained by plotting the fraction of olefins in the $C_2$ and $C_3$ fractions. Unsaturation decreased with increasing hydrogen content of the feed and with increasing conversion. At conversions greater than 0.15 to 0.2 the $H_2$-CO ratio of the exit gas increased with increasing conversion for all of the feed gases except $0.25H_2+1CO$. Plots of unsaturation against the ratio of $H_2$ to $(H_2+CO)$ of the exit gas showed a fair overall relationship of decreasing unsaturation with increasing hydrogen content. However, this plot consisted principally of four clusters of points corresponding to the four feed gases and poor correlation existed within points for a given feed gas. Thus, the plots in figure 13 are considered the best representation of these data.

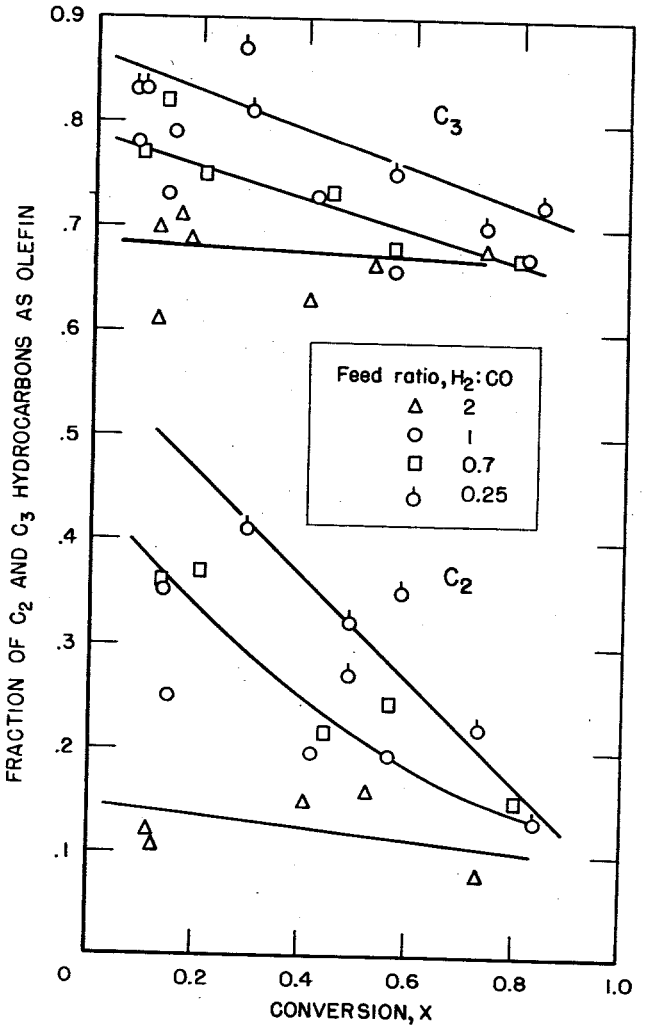


FIGURE 13.—Olefins in $C_2$ and $C_3$ Fractions as a Function of Conversion for Nitrided Catalyst D3001 at 225° C and 21.4 Atmospheres.

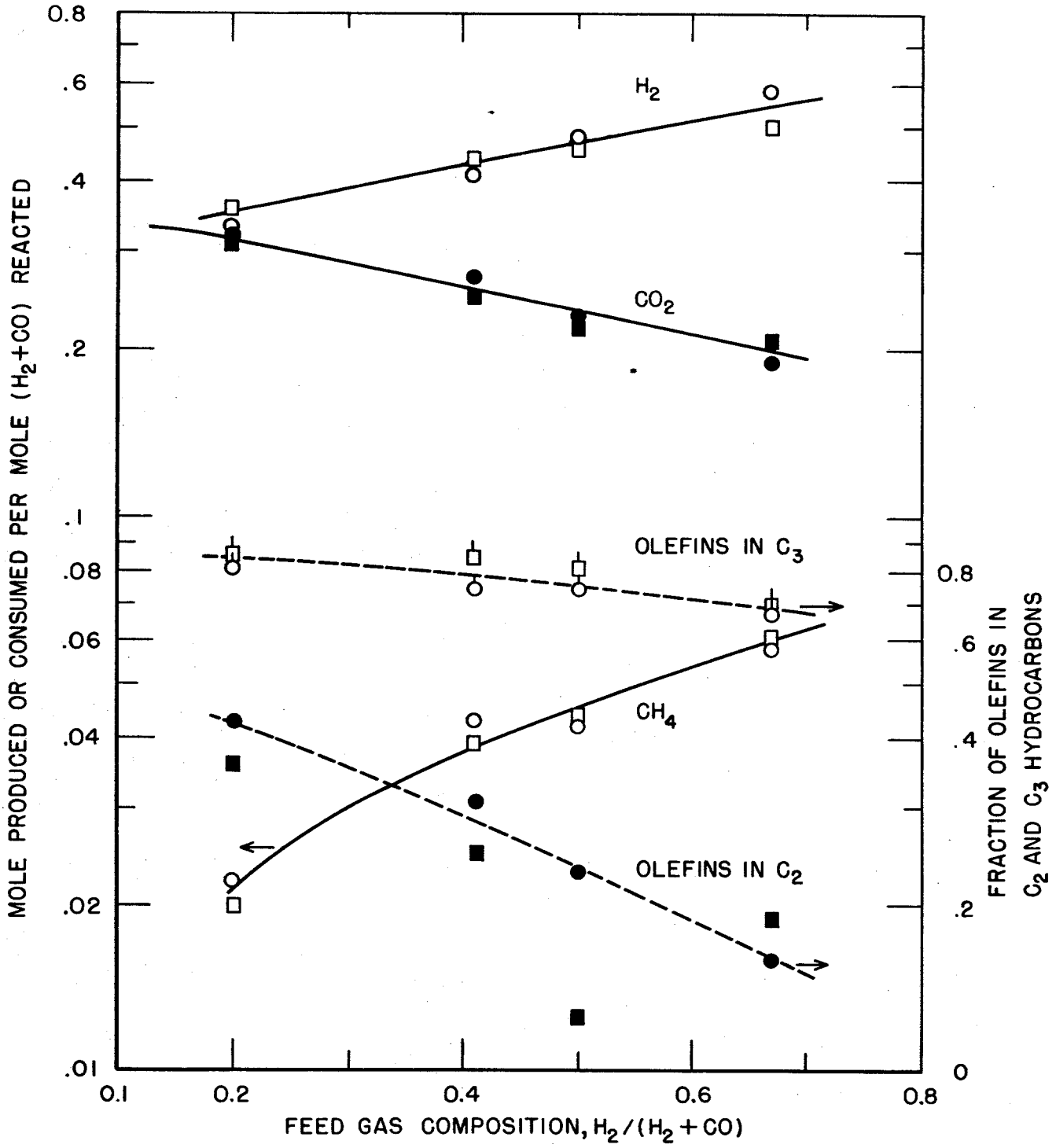


FIGURE 14.—Selectivity as a Function of Feed Gas Composition, at 21.4 Atmospheres and Conversion of 30 Percent. Circles represent 225°C and squares 240°C.

Figure 14 compares selectivity data for 225° and 240° C at a conversion of 30 percent with the feed composition.

Pressure has only a small influence on selectivity, as indicated by the tests of nitrided iron catalyst D3001 with $1H_2+1CO$ gas at 240° C and 7.8 to 21.4 atmospheres; the rate data for these tests were described in the previous section. As shown in figure 15, the relative usage of hydrogen was essentially the same, except for the somewhat higher values at 7.8 atmospheres for conversions below 0.5. Methane production decreased with increasing pressure; for example, the values of $m_{CH_4}/x$ at a conversion of 0.4 were 0.053, 0.047, 0.043, and 0.043 at 7.8, 11.2, 14.6, and 21.4 atmospheres, respec-

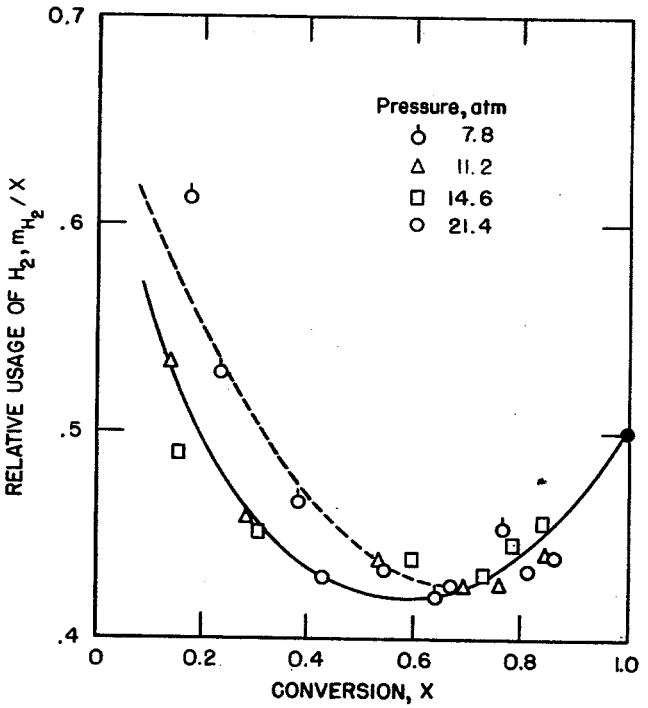


FIGURE 15.—Relative Usage of Hydrogen as a Function of Conversion and Operating Pressure. $1H_2+1CO$ Gas at 240° C.

tively. Unsaturation and $CO_2$ production were essentially the same at all pressures.

Previous investigators (*8,36,62*) have postulated that the primary synthesis reaction produces water, $m_{H_2}/x=0.67$, and that carbon dioxide is produced by a subsequent water-gas-shift reaction. The present data can be explained by this hypothesis. As relative $H_2$ consumption and $CO_2$ production are essentially independent of temperature and pressure and are functions only of conversion and feed composition, as shown by the present and previous data, the subsequent water-gas-shift must vary in approximately the same manner as the rate of synthesis when pressure and temperature are changed. The rate equation of Kul'kova and Temkin (*43*) for the water-gas-shift on iron

$$r_{wg}=k_1[p_{CO}(p_{H_2O}/p_{H_2})^{1/2}-(1/K)p_{CO_2}(p_{H_2}/p_{H_2O})^{1/2}] \quad (15)$$

where $r_{wg}$ is the differential reaction rate, $k_1$ is a rate constant with an activation energy of 16.5 kcal/mole, $K$ is the equilibrium constant, has the same pressure dependence as the synthesis and nearly the same temperature dependence. Activation energies for synthesis vary from 19 to 23 kcal/mole.

The differential product of $CO_2$ may be related to $r_{wg}$ as

$$dm_{CO_2}/dx=[dm_{CO_2}/d(1/S)]/[dx/d(1/S)]=r_{wg}/r_{syn} \quad (16)$$

where $S$ is the space velocity of feed gas and $r_{syn}$ is the rate of synthesis. Calculations based on equation (16) show at least a qualitative agreement between $CO_2$ production and equation (15); however, the present experimental data are not sufficiently precise to provide a positive test. Thus, the Temkin equation provides at least a first approximation to the kinetics of $CO_2$ production in the Fischer-Tropsch synthesis on iron.

Recent kinetic studies of the water-gas-shift on iron catalysts have led to different equations than Temkin (*43*) reported. Krusenstierna (*42*) observed that the rate of the forward reaction was directly proportional to partial pressure of CO, independent of water vapor except at very low concentrations, independent of $H_2$, and inhibited moderately by $CO_2$. Mars, Gorgels, and Zwietering (*45*) confirmed the observations of Krusenstierna, and an activation energy of about 27 kcal/mole was reported. Bohlbro (*15*) analyzed kinetic data at 1 and 20 atmospheres in terms of an equation of the form $r=kp_{CO}{}^{l}p_{H_2O}{}^{m}p_{CO_2}{}^{n}p_{H_2}{}^{q}$ for the forward reaction. Exponents were found to have the following values: $l=0.8$–$1.0$; $m=0.2$–$0.35$; $n=-0.65$ to $-0.5$; and $q=0$. For the equation of Bohlbro the rate increases with operating pressure to 0.6 to 0.7 power. This equation would probably also explain $CO_2$ formation in the Fischer-Tropsch synthesis.

The production of $CO_2$ could also result entirely or in part from reactions coupled with the primary synthesis mechanism, such as the reaction of water vapor with an intermediate of the synthesis. Water-gas-shift equilibrium is usually not attained during synthesis on iron, and tests with $C^{14}O_2$ added to $1H_2+1CO$ feed indicate that the reverse shift and the direct synthesis from $CO_2$ proceed very slowly (*26*). One cannot distinguish here between mechanisms involving irreversible reactions and slow reverse reactions. For example, for typical concentrations of reactants and products from iron catalysts the forward reaction according to equation (15) is about 50 times faster than the reverse shift.

Methane is a primary product of the synthesis. Its production increases with $H_2$-CO ratio of the feed; however, at low conversions $CH_4$ production, $m_{CH_4}/x$, decreases with increasing conversion, although the $H_2$-CO ratio of the gas remaining increases. Inhibition of $CH_4$ production may possibly be attributed to water vapor. At higher conversions, the effect of the increasing inhibitor concentration is outweighed by the increasing $H_2$-CO ratio of the gas remaining, and $CH_4$ production passes through a minimum and increases.

Olefins are also primary products of the synthesis, and olefin production decreases with increasing $H_2$-CO ratio of the feed gas (*44*).

TABLE 4.—*Comparison of results of iron and cobalt catalysts*

[Conversion=0.3]

| | Iron catalysts * | | | Cobalt catalysts † | | |
|---|---|---|---|---|---|---|
| Feed gas | $2H_2+1CO$ | $1H_2+1CO$ | $0.25H_2+1CO$ | $3.5H_2+1CO$ | $2H_2+1CO$ | $1H_2+1CO$ |
| Relative $H_2$ usage, $m_{H_2}/x$ | 0.54 | 0.47 | 0.34 | 0.70 | 0.70 | 0.67 |
| $CO_2$ production, $m_{CO_2}/x$ | .200 | .225 | .31 | .003 | .019 | .033 |
| Methane production, $m_{CH_4}/x$ | .059 | .046 | .021 | .059 | .041 | .025 |
| Unsaturation‡ | .69 | .77 | .84 | .45 | .66 | .71 |

* Reduced and nitrided $Fe_3O_4$-MgO-$K_2O$ catalyst at 21.4 atmospheres and 225°–240° C.
† Reduced Co-$ThO_2$-kieselguhr catalyst at atmospheric pressure and about 195° C.
‡ Unsaturation is given as the fraction of olefins in $C_3$ fraction for iron catalysts and in $C_4$ fraction for cobalt.

Olefin production decreases with increasing conversion and with increasing $H_2$-CO ratio of the exit gas, which also usually increases with increasing conversion; however, the $H_2$-CO ratio is not the only factor determining unsaturation. A complete explanation of olefin production probably involves the hydrogenation of olefins in subsequent parts of the catalyst bed.

The present results with iron catalysts may be compared with similar data from this laboratory on cobalt catalysts at atmospheric pressure and 190° to 205° C with feed gases of composition $3.5H_2+1CO$ and $1H_2+1CO$ (*6*). For cobalt catalysts, the relative usage of hydrogen was about 0.70 and was essentially independent of temperature, feed gas, and conversion. The production of $CO_2$ on cobalt was about 10 percent of that on iron, but apparently most of the $CO_2$ was also produced by a subsequent water-gas-shift reaction. Carbon dioxide formation increased with increasing carbon monoxide content of feed, conversion, and temperature. Methane production increased with $H_2$-CO ratio of feed and with temperature. Unsaturation of the $C_4$ fraction decreased with increasing $H_2$-CO ratio of the feed, but appeared to be largely controlled by the $H_2$-CO ratio of the gas remaining. Thus, for the hydrogen-rich gases, the $H_2$-CO ratio of gas remaining increased, and unsaturation decreased with increasing conversion. For $1H_2+1CO$ feed, the $H_2$-CO ratio decreased, and the unsaturation increased with increasing conversion. Selectivity data for iron and cobalt catalysts are compared at a conversion of 0.3 in table 4.

## EFFECT OF WATER VAPOR, CARBON DIOXIDE, METHANE, AND ARGON ON RATE

In the water addition experiments (*33*), as in the preceding sections, the conversion, $x$, is defined as moles of $H_2+CO$ consumed per moles of $H_2+CO$ feed, and space velocity as volumes (STP) of $H_2+CO$ fed per bulk volume of catalyst per hour. Water concentration in the feed is expressed as mole-percent of water based on moles of $H_2+CO$ feed.

Experiments were made with 6- to 8-mesh nitrided iron catalyst D3001 at 21.4 atmospheres and 240° C with $1H_2+1CO$. Tests at hourly space velocities from 100 to 900 were made with 0, 10, 20, and 30 mole-percent water vapor.

As the present experiments were made to demonstrate the immediate effects of water vapor, periods of water addition were always less than 8 hours. The catalyst was operated at 240° C and an hourly space velocity of about 300 for 16 days before the kinetics tests were begun and between periods of water addition. Intermediate synthesis at the reference conditions without added water for at least 16 hours provided a check on the constancy of catalytic activity. The same charge of catalyst was used in all water-addition experiments.

For each water test the space velocity was changed to the desired value and water was added. Kinetic data were obtained during 2 hours of operation when gas flows were measured and gas samples were collected over mercury for analysis. After the test period the flow of water was stopped, and the hourly space velocity was adjusted to 300.

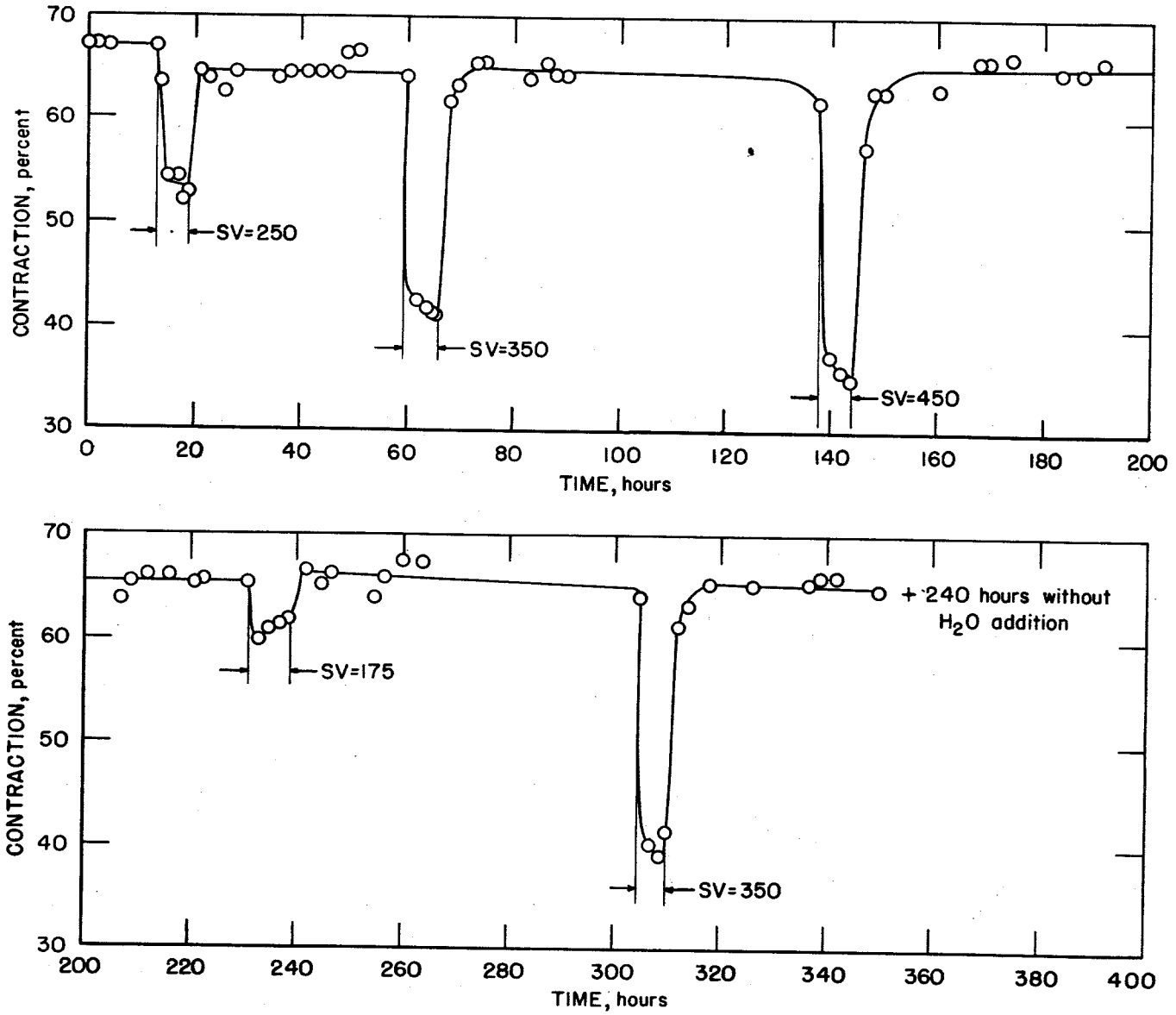


FIGURE 16.—Contraction ($CO_2$-Free) During Initial Period of Synthesis at 240° C and 21.4 Atmospheres With $1H_2+1CO$.

Figure 16 presents a plot of $CO_2$-free contraction as a function of time for the first several periods of water addition. In every case the contraction decreased abruptly and attained an essentially constant value in 1 to 3 hours. Although small variations in contraction occurred during the test period, these usually do not exceed the reproducibility of contraction values, $\pm 0.5$, in these experiments. When water addition was stopped and the flow readjusted, the contraction usually regained its initial value of 65 percent $\pm$ 2 percent in a few hours. In a few periods the contraction under reference conditions was 60 percent. At the end of the experiment, after a total of 110 days of synthesis, contraction under reference conditions was 63 percent. These data indicate that the variations in rate and selectivity were kinetic effects of water vapor and were not caused by progressive permanent changes in the catalyst.

Primary data for tests with 10 and 30 mole-percent water vapor are presented in figures 17 and 18. In the upper blocks the fraction of $H_2+CO$ converted, $x$, and the space-time yield, $xS$, are plotted as functions of reciprocal space velocity ($1/S$) of $H_2+CO$ feed. The mole fractions of the principal gaseous components are shown in the lower block. For the addition of 20 and 30 percent water vapor, the concentration of water decreased with increasing conversion, but for addition of 0 and 10 percent water vapor its concentration increased with conversion. For all feed compositions the concentration of carbon monoxide decreased rapidly with

increasing conversion. With increasing conversion the concentration of hydrogen decreased monotonically for zero $H_2O$ addition, but in water-addition experiments the concentration of $H_2$ increased to a maximum and then decreased.

Figure 19 presents double logarithmic plots of the conversion of $H_2+CO$ (lower block) and of CO (upper block) as a function of reciprocal space velocity of $H_2+CO$ for various quantities of added water. At the same space velocity the conversion of $H_2+CO$ decreases with increasing concentrations of water vapor in the feed, but the conversion of CO is approximately constant. The first- and half-order empirical equations described previously (p. 8), fit the data for conversion of $H_2+CO$ moderately well, and these equations yield extrapolated values for the differential reaction rate at

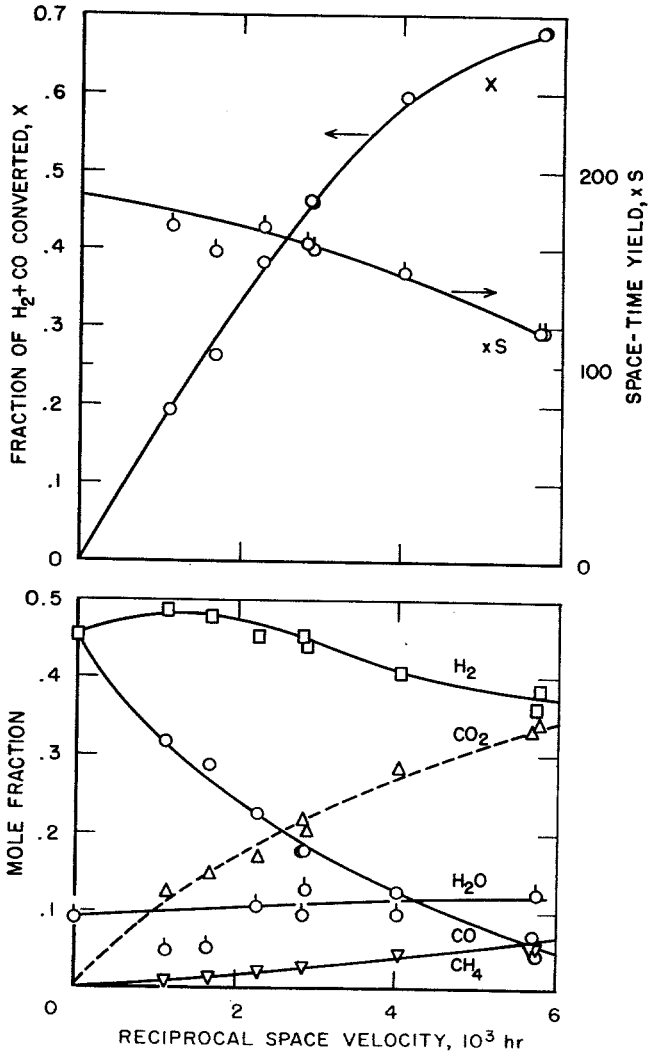


FIGURE 17.—Kinetic Data for Synthesis on Nitrided Iron Catalyst With $1H_2+1CO$ Gas+10 Mole-percent $H_2O$ at 21.4 atmospheres and 240° C.

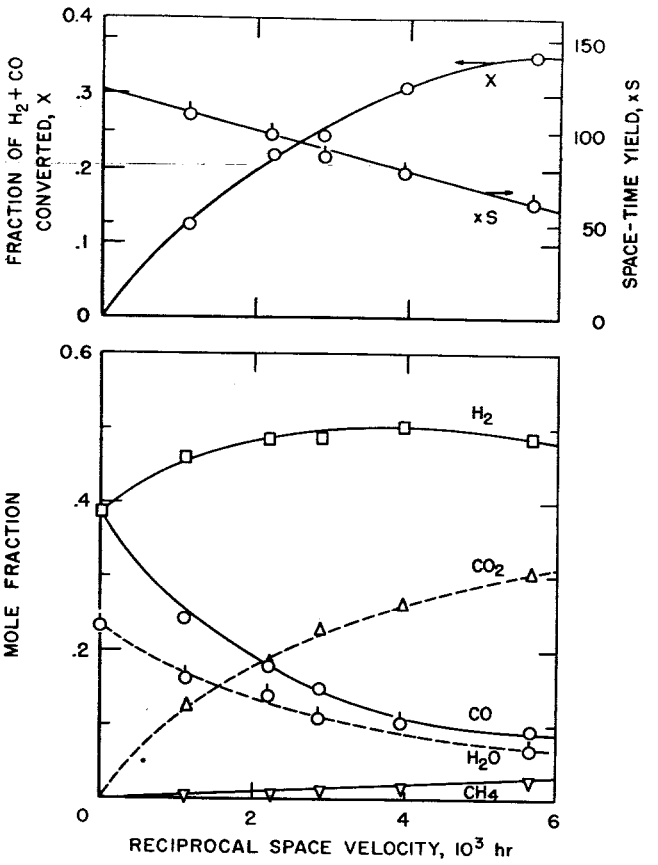


FIGURE 18.—Kinetic Data for Synthesis on Nitrided Iron Catalyst With $1H_2+1CO$ Gas+30 Mole-percent $H_2O$ at 21.4 atmospheres and 240° C.

$x=0$, $r_0$, which can be correlated with the feed composition. Table 5 presents values of $r_0$ in terms of $H_2+CO$ converted for experiments with various quantities of added water. The values of $r_0$ estimated from the two empirical equations agree within 5 percent. As the initial rate of synthesis in tests without water addition has been shown to be proportional to the partial pressure of synthesis gas, $p_{sg}$, the average values of initial reaction rates have

TABLE 5.—*Initial reaction rate as a function of water added to feed*

[240° C., 21.4 atmospheres, $1H_2+1CO$ feed]

| Water added, mole-percent | Partial pressure of $H_2O$, atmospheres | Initial reaction rate, $r_0$ * | | $r_0$ (average) † |
|---|---|---|---|---|
| | | One-half order | First order | $p_{sg}$ |
| 0 | 0 | 298 | 285 | 13.6 |
| 10 | 1.95 | 192 | 201 | 10.1 |
| 20 | 3.57 | 165 | 160 | 9.15 |
| 30 | 4.94 | 121 | 102 | 6.73 |

* Cubic centimeters (STP) of $H_2+CO$ reacted per cubic centimeter of catalyst per hour.

† Average of values in columns 3 and 4 divided by $p_{sg}$, the partial pressure of synthesis gas in atmospheres.

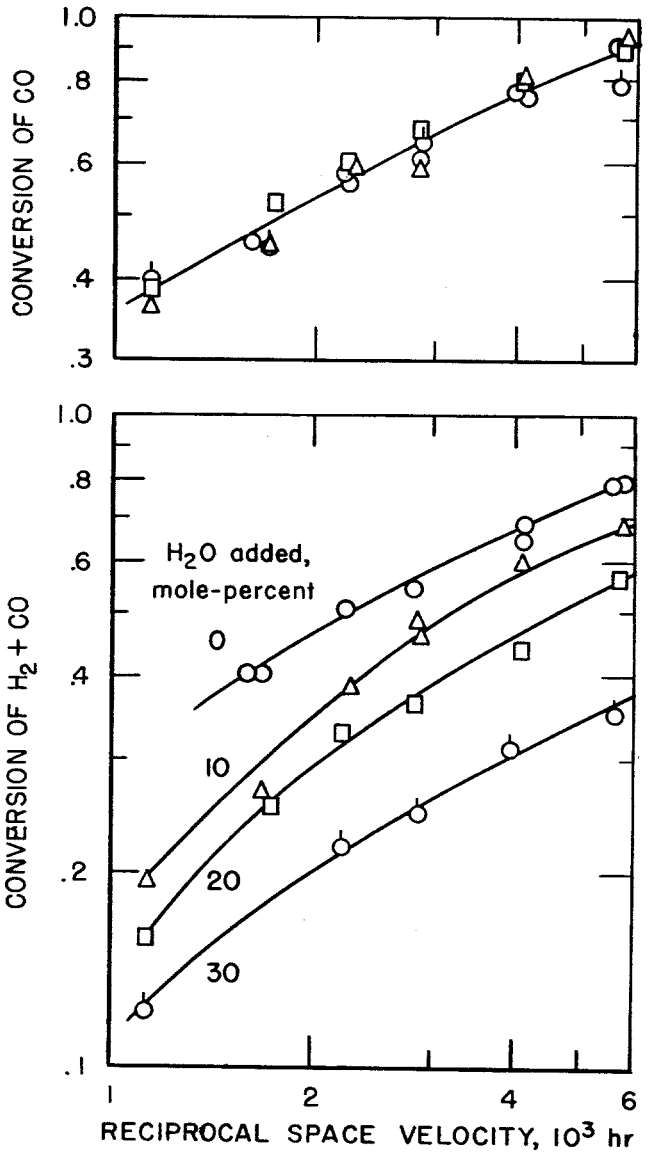


FIGURE 19.—Double Logarithmic Plots of Conversion of $H_2+CO$ and CO as a Function of Reciprocal Space Velocity in $H_2O$ Addition Tests With $1H_2+1CO$ at 21.4 Atmospheres and 240° C.

been divided by partial pressure of synthesis gas in the feed in the last column of the table. The values of both $r_0$ and $r_0/p_{sg}$ decrease sharply with increasing partial pressure of water vapor.

Figures 20 to 22 present selectivity data in terms of moles of $H_2$ consumed and $CO_2$ or $CH_4$ produced per mole of $H_2+CO$ consumed. These data are of the form $m_i/x$, where $m_i$ is the moles of component $i$ consumed or produced per mole of $H_2+CO$ feed, and $x$ is conversion of $H_2+CO$ as previously defined. Included on these graphs are data (solid circles) for synthesis with $1H_2+1CO$ at 240° C on another sample of the same catalyst (*32*). These points serve to define the selectivity over a wider range of conversion. When water was added to the feed, the relative usage of hydrogen (fig. 20) decreased with increasing water content of the feed, and for a given concentration of water vapor the usage increased sharply with conversion. The shapes of the curves for water addition are completely different from those obtained when no water was added. For high concentrations of water vapor, a net production of hydrogen was observed so that the overall reaction involved the $H_2O+CO$ synthesis as has been reported by Kölbel (*37–40*).

Carbon dioxide production (fig. 21) varied inversely to hydrogen usage (fig. 20). Carbon dioxide production increased with increasing water in the feed and with decreasing conversion. For purposes of comparison it may be assumed that all $CO_2$ is produced by the water-gas shift and that the value of 0.33 $CO_2$ per $H_2+CO$ consumed corresponds to the water-gas shift and synthesis proceeding at the same rates. On this basis the water-gas shift proceeded about four times as rapidly as the primary synthesis reactions when 30 mole-percent water was added.

When water was added to the feed, methane production (fig. 22) increased rapidly with increasing conversion. The slopes of the curves

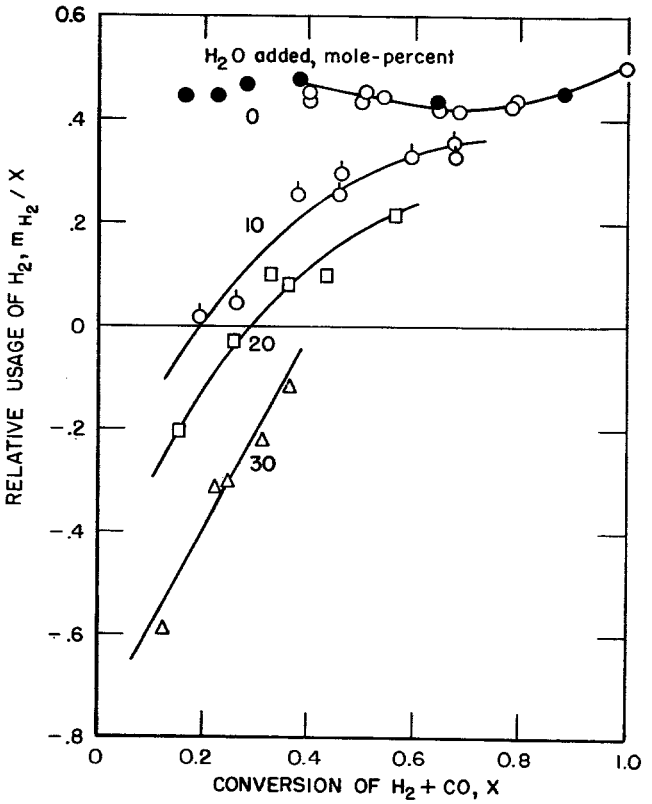


FIGURE 20.—Relative Usage of Hydrogen as a Function of Conversion and Added Water at 21.4 Atmospheres and 240° C.

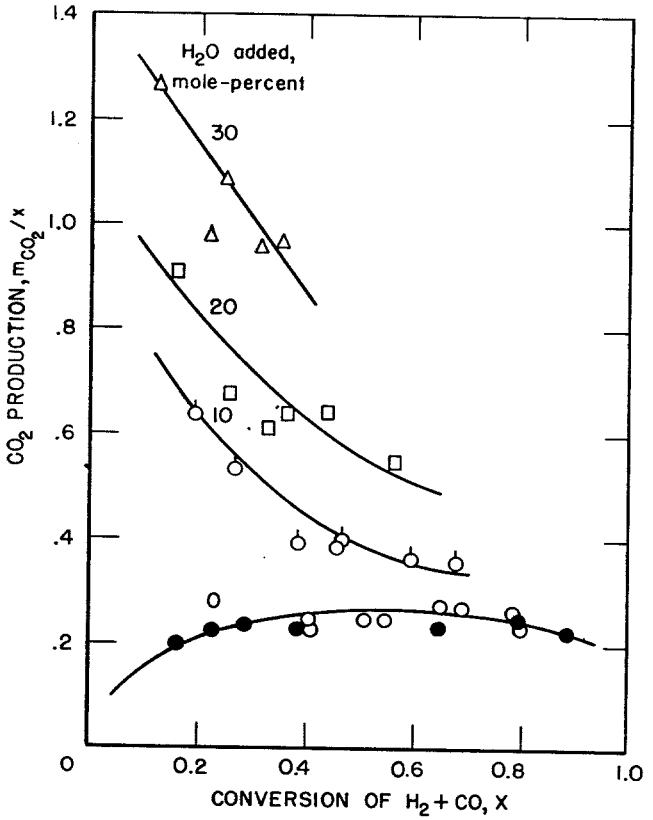


FIGURE 21.—Production of $CO_2$ as a Function of Conversion and Added Water at 21.4 Atmospheres and 240° C.

increased with increasing concentration of water in the feed, probably because of the increased $H_2$-CO ratios of the gas reacting. Because less methane is produced at low conversions when water is added, water must inhibit methane formation; however, with increasing conversion the rapidly increasing ratio of $H_2$ to CO and the decreasing concentration of water vapor cause the rapid increase in methane formation shown in figure 22.

A number of experiments were made with a second sample of 6- to 8-mesh nitrided catalyst D3001 to determine the effects of an inert component, argon, and two of the products of the reaction, $CO_2$ and $CH_4$, on the rate of synthesis at an operating pressure of 7.8 atmospheres. Two calibrated flowmeters were used to regulate the flows of $1H_2+1CO$ gas and the diluent. The space velocity of synthesis gas was maintained constant and the flow of the diluent was increased stepwise until its flow was about three times the flow of synthesis gas. The lower pressure was used in these tests because of limitations of the flowmeters employed. Previous studies have shown that the kinetics are essentially the same in this range of pressure (*32*).

This straightforward design of experiment yields data that are difficult to interpret quantitatively; however, for comparative purposes they are adequate, as one of the diluents, argon, can be assigned the role of an inert component.

The effects of argon, $CH_4$, and $CO_2$ as diluents are compared with those of water in figure 23, where a measure of catalytic activity, $-S\ ln(1-x)$, is plotted as a function of the partial pressure of $H_2+CO$ in the feed. Plots of this type for the variation of activity with pressure of $1H_2+1CO$ feed (no diluent) are linear and have a slope of about unity (*8*). The rate of synthesis decreases at about this rate when $CO_2$ is added to the feed. The rate decreases less rapidly for the addition of argon and $CH_4$, and more rapidly for water vapor. Also plotted on figure 23 are data read from a graph in the paper of Tramm (*63*). Experimental conditions were not stated by Tramm and the following values were assumed: Pressure, 25 atmospheres, and hourly space velocity, 100. Although the data of Tramm were probably obtained on a reduced precipitated iron catalyst, his results are similar to ours.

Although the results of experiments such as shown in figure 23 cannot be quantitatively interpreted, argon can be a diluent only. As the data for methane and argon are similar, methane may also be regarded as an inert component. Both carbon dioxide and water are inhibitors because the rate decreased more

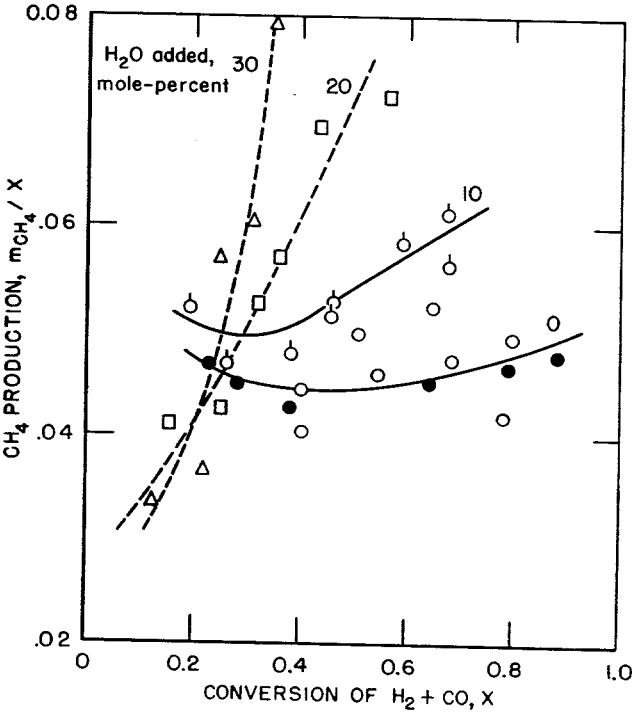


FIGURE 22.—Production of Methane as a Function of Conversion and Added Water Vapor at 240° C and 21.4 Atmospheres.

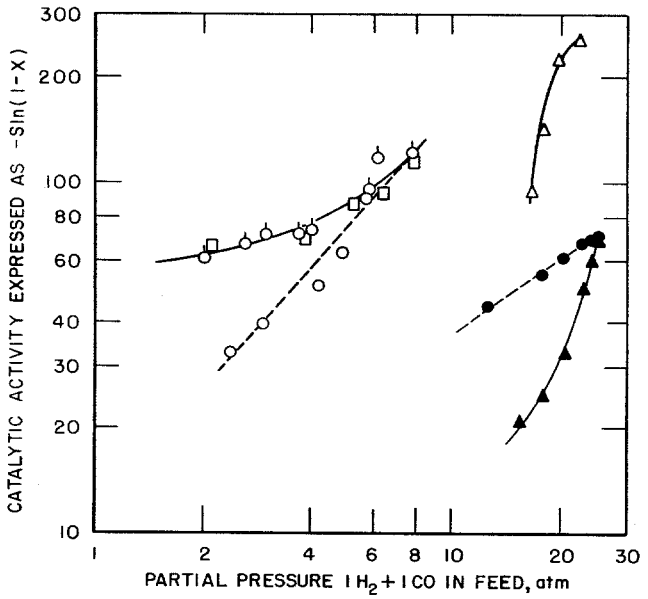


| Symbol | Diluent | Temperature, °C | Pressure, atm |
|---|---|---|---|
| ○ | $CO_2$ | 229 | 7.8 |
| ◑ | $CH_4$ | 220 | 7.8 |
| □ | A | 224 | 7.8 |
| △ | $H_2O$ | 240 | 21.4 |
| Data of Tramm ▲ | $H_2O$ | ? | 25.0(?) |
| Data of Tramm ● | $CO_2$ | ? | 25.0(?) |

FIGURE 23.—Double Logarithmic Plots of Activity Against Partial Pressure of $1H_2+1CO$ in Feed in Dilution Tests.

rapidly with increasing concentrations of these components than with argon. Compared with water vapor, carbon dioxide has only a slight inhibiting effect.

Although water vapor severely decreases the rate of synthesis, it is an inhibitor or temporary poison because catalytic activity is promptly restored when the addition of water vapor is stopped. Other experiments in our laboratory have shown that prolonged exposure of the catalyst to high concentrations of water vapor or $CO_2$ during synthesis will lead to permanent loss in activity as has been reported by Tramm (*63*).

The initial rates for the water addition experiments can be approximated by a Langmuir-type equation of the form $r=a\,p_{sg}/(1+b\,p_{H_2O})$, where $p_{sg}$ and $p_{H_2O}$ are the partial pressures of $H_2+CO$ and water vapor, respectively, and $a$ and $b$ are constants. However, this equation does not properly express the linear dependence of rate on operating pressure. Equations of the types, $r=a\,p_{sg}/(1+b\,n_{H_2O})$ or $r=a\,p_{sg}-b\,p_{H_2O}$, where $n_{H_2O}$ is the mole fraction of water, provide the proper dependence on concentration of water vapor and total pressure.

No appreciable change in the rate of consumption of carbon monoxide was noted with water addition. This observation suggests that the activation of carbon monoxide may be the rate-determining step in the process, and that the subsequent reactions of carbon monoxide to produce hydrocarbons or carbon dioxide are relatively unimportant to the rate.

With higher concentrations of added water, hydrogen is produced in the synthesis and the net reaction is a $H_2O+CO$ synthesis as described by Kölbel (*37–40*). When water is added, the water-gas shift proceeds rapidly. If the primary synthesis reactions produce water, the shift reaction—when 30 mole-percent water is added—is four times as fast as synthesis. When water is added, the relative usage of hydrogen increases rapidly with increasing conversion of $H_2+CO$ and for a given conversion this quantity decreases with increasing concentration of water in the feed. The production of $CO_2$ varies in an opposite manner. Although the accuracy of the data does not permit a detailed analysis of the rate of the water-gas shift or other reactions that may produce $CO_2$ such as a Kölbel-type synthesis, the production of $CO_2$ increases with increasing concentrations of $H_2O$ and CO. The rate equation of Temkin seems to be a first approximation (*43*).

Kölbel and coworkers (*40*) proposed an empirical rate equation for the consumption of CO in the $H_2O$-CO synthesis in the form

$$r_{CO}=13p_{CO}^{0.5}p_{H_2O}^{0.2}+3p_{CO}^{0.2}p_{H_2}^{1.5}. \qquad (17)$$

This equation expresses the overall consumption of CO in all processes; for example, a water-gas-shift followed by the usual synthesis reactions. For the present data, as shown in figure 19, $r_{CO}$ is essentially independent of water addition, and it may be assumed that $r_{CO}$ is also independent of water addition at zero conversion, where the gas composition is that of the feed. Feed compositions for our water addition experiments were substituted in equation (17) and computed values of $r_{CO}$ were constant to within $\pm 10$ percent. Thus, equation (17) appears to be valid as an empirical expression for the overall rate of CO consumption, but this equation does not properly express the pressure dependence of rate.

Methane production is drastically affected by water vapor. Previous studies had already suggested that methane production was decreased by water vapor and increased by increasing the $H_2$-CO ratio of the gas. The initial decrease may be attributed to the inhibiting effect of water. However, the $H_2$-CO ratio of the gas increases rapidly with increas-

ing conversion, and the concentration of water either remains essentially constant or decreases. The inhibiting effect of water vapor is soon outweighed by the increasing ratio of $H_2$ to CO, and methane production increases with conversion.

## A SEMIFUNDAMENTAL RATE EQUATION FOR THE FISCHER-TROPSCH SYNTHESIS ON IRON CATALYSTS

The analyses of kinetic data in preceding sections have shown that the initial reaction rate $r_0$ in terms of $H_2+CO$ consumed can be approximated by

$$r_0=k_1 p_{H_2}{}^n p_{CO}{}^{1-n} \tag{18}$$

where $k_1$ is a rate constant with an activation energy of about 20 kcal/mole, $p_{H_2}$ and $p_{CO}$ are, respectively, the partial pressures of hydrogen and carbon monoxide, and $n$ is about 0.66 (*31*). In general, the rate may be approximated by $r=f(x)g(P)h(T)$, where $f(x)\sim(1-x)^{0.5 \text{ to } 1.0}$, $g(P)\sim P$, and $h(T)\sim\exp(-20 \text{ kcal mole}^{-1}/RT)$; in these expressions $x$ is the fraction of $H_2+CO$ reacted and $P$ the operating pressure. The function $f(x)$ may be approximated by $n_g/(1+bn_{H_2O})$ or by $n_g(1-cn_{H_2O})$ where $n_g$ and $n_{H_2O}$ are the mole fractions of $H_2+CO$ and water vapor, respectively, and $b$ and $c$ are constants (*32*). The equations of Tramm (*62*) have as their principal terms $p_{H_2}{}^n p_{CO}$, where $n$ is 1 or 2. This expression does not fit the data from Bureau of Mines experiments with fused iron catalysts. The equations of Uchida (*64*) fail to express the variation of rate with operating pressure.

Experiments in which water vapor, $CO_2$, and $CH_4$ were added to the feed indicate that water vapor and $CO_2$ are, respectively, strong and weak inhibitors or temporary poisons and that $CH_4$ is only a diluent (see preceding section).

In the present section a rate equation is developed in terms of fractional coverages of the surface by reactants and products (*5*). These surface coverages are then approximated by Freundlich isotherms; that is, the coverage by component $i$ is proportional to the partial pressure of $i$ to a positive exponent less than one. This approximation has been shown to be valid in a number of systems (*17, 57, 67*). Exponents of the partial pressure terms were adjusted to make the equation consistent with observations cited in the first paragraph of this section, and the equation was tested in a differential form.

A semifundamental rate equation was developed based on a simplified version of the scheme of chain growth postulated by Storch, Golumbic and Anderson (*60*). An intermediate $C_1$ of the type 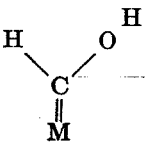 is formed on the catalyst surface by the reaction of adsorbed H and CO. Intermediate $C_1$ reacts with other intermediates $C_1$, $C_2$ . . . . . $C_n$ to form the next higher intermediate or is removed by reaction with water vapor, according to

$$2H_{ads}+CO_{ads}\rightarrow C_1 \tag{19}$$

$$\begin{aligned} C_1+C_1&\rightarrow C_2+H_2O\\ C_1+C_2&\rightarrow C_3+H_2O\\ &\vdots\quad\quad\vdots\\ C_1+C_n&\rightarrow C_{n+1}+H_2O \end{aligned} \tag{20}$$

$$C_1+H_2O_{ads}\rightarrow 2H_2+CO_2. \tag{21}$$

Intermediates $C_i$ desorb from the surface at a rate proportional to their concentration to form product of carbon number $i$. According to previous chain growth postulates (*21*) $C_n\cong C_1\alpha^{n-1}$, where $\alpha$ is a constant, $0<\alpha<1$, and $\sum_1^\infty C_1=C_1/(1-\alpha)=C_1 g$, where $g=1/(1-\alpha)$.

Reactions (19), (20), and (21) are postulated to control the rate of synthesis. The rate of formation $C_1$ is given as

$$r_1=a\theta_H{}^2\theta_{CO} \tag{22}$$

and the rate of removal of $C_1$ by equations (20) and (21)

$$r_{2,3}=b\theta_1\left(\sum_1^\infty \theta_i\right)+c\theta_1\theta_{H_2O} \tag{23}$$

$$=b\theta_1{}^2 g+c\theta_1\theta_{H_2O} \tag{24}$$

where $a$, $b$, and $c$ are rate constants, and $\theta_H$, $\theta_{CO}$, $\theta_{H_2O}$, $\theta_1$, and $\theta_i$ are, respectively, the fractional coverage of the surface by hydrogen atoms, CO, $H_2O$, $C_1$ and $C_i$ intermediates. For steady-state conditions, $r_1=r_{2,3}$ and

$$a\theta_H{}^2\theta_{CO}=bg\theta_1{}^2+c\theta_1\theta_{H_2O}. \tag{25}$$

The rate of synthesis measured in terms of $H_2+CO$ consumed (or hydrocarbon produced) may be given as

$$r=bg\theta_1{}^2 \tag{26}$$

and from equation (25)

$$r=a\theta_H{}^2\theta_{CO}-c\theta_1\theta_{H_2O} \tag{27}$$

$$=a\theta_H{}^2\theta_{CO}-(c/\sqrt{bg})r^{1/2}\theta_{H_2O}. \tag{28}$$

It is now assumed that surface coverages may be approximated by $\theta_j=m_j p_j{}^{n_j}$, where $m_j$ and $n_j$ are constants ($0<n_j<1$) and $p_j$ is the partial pressure of component $j$. The exponents of these Freundlich isotherms are adjusted to provide the observed dependence of rate on

total pressure and on gas compositions, leading to a final equation

$$r = a' p_{H_2}^{0.6} p_{CO}^{0.4} - f' r^{0.5} p_{H_2O}^{0.5} \quad (29)$$

where $a' = a m^2_H m_{CO}$ and $f' = c m_{H_2O}/\sqrt{bg}$. The exponents of $p_{H_2}$ and $p_{CO}$ differ slightly from those derived previously and were chosen by trial and error to provide better agreement with available experimental data.

The integration of rate equation (29) is virtually impossible, especially because the usage ratio of $H_2$ to CO is not constant. Therefore, the rate data were differentiated to yield the differential reaction rate. The rate equation was then tested in the linear form

$$p_{H_2}^{0.6} p_{CO}^{0.4}/r = (1/a') + (f'/a') p_{H_2O}^{0.5}/r^{0.5}. \quad (30)$$

Differential reaction rates were obtained by numerical or graphical differentiation of data reported previously for synthesis on 6- to 8-mesh nitrided iron catalysts D3001 with feed gas ratios of $H_2$ to CO of 2, 1, 0.7 and 0.25 at 21.4 atmospheres and 225° and 240° C. Smooth curves were passed through plots of conversion of $H_2+CO$, $x$, as a function of reciprocal hourly inlet space velocity, $S^{-1}$, for each set of experimental data, and values of x were read from the curves at small equal intervals of $S^{-1}$.

Two methods of differentiation were used. In the first, at each point a four-constant polynomial was fitted to the reference point and three equal intervals immediately above and below it by a central difference equation involving least squares methods. (A 6-constant equation could be fitted exactly to the 7 points; however, this equation would accentuate fluctuations of the data, and would represent the trend of the curve less satisfactorily.) The differential reaction rate, $r = dx/dS^{-1}$ at the reference point, is then given by the coefficient of the second term of the polynomial. The second method used log-log plots as described previously (*2*). The results by the two methods were essentially the same except for conversions greater than 0.6, where the log-log method became difficult to apply. Derivatives obtained for known curves usually deviated from actual values by less than 3 percent. Values of $r$ at zero conversion were averages obtained from one-half and first-order empirical equations.[5] The numerical differentiation resulted in smooth plots of the derivatives as a function of conversion as shown in figure 24. Plots of equation (30) were made from these values of $r$ and partial pressures of $H_2$, CO and $H_2O$, as shown in figure 25, where the positions of the lines were determined by least squares. As the values of rate and partial pressure of water vapor have uncertainties of about ±5 percent, the equation is considered to be a satisfactory representation of the data. Also plotted on figure 25 are three points for initial reaction rates obtained from water addition experiments at 240° C (see preceding section). These values obtained with a different charge of the same catalyst agree reasonably well with data from experiments in which no water was added. Values of constants of equation (29) and activation energies are given in table 6. The activation energy of constant $a'$ is similar to that obtained by empirical methods (*31*). At low to moderate conversions the rate is determined principally by the first term of equation (29).

TABLE 6.—*Constants of equation (29) for synthesis on nitrided, fused iron catalyst D3001 at 21.4 atmospheres*

| | Temperature ° C. | | Activation energy kcal/mole |
|---|---|---|---|
| | 225 | 240 | |
| a′ ($atm^{-1}$ $hr.^{-1}$) | 15. 2 | 27. 6 | 20. 2 |
| f′ ($atm^{-½}$ $hr.^{-½}$) | 1. 67 | 2. 87 | 18. 5 |

As a test of the accuracy of equation (29), values of $r$ were computed for each of the points in figure 24 using constants in table 6, and the relative error, $(r_c - r_{obsd})/r_{obsd}$ where $r_c$ and $r_{obs}$ are, respectively, the calculated and observed values of the differential reaction rate, was computed. Five of the 49 calculated values, all at relatively high conversions, deviated from the observed by more than 20 percent. For the remainder, the average of absolute values of relative error was 5.5 percent. In addition, systematic deviations were noted. For feed gases containing $2H_2+1CO$ and $0.25H_2+1CO$, calculated rates were smaller than observed, and for $0.7H_2+1CO$ they were larger. Changing the exponents of the first term of equation (29) from $p_{H_2}^{0.6} p_{CO}^{0.4}$ to $p_{H_2}^{0.66} p_{CO}^{0.34}$ improved the plots somewhat for all feed gases except $0.25H_2+1CO$, but for this feed gas deviations from the best line were much larger. The exponents used in equation (29) seem to be the best choice.

In developing equation (29) the production of all of the $CO_2$ was not ascribed to reaction (21). In equation (29) the first term is a measure of the total CO consumed and the second term is the CO converted to $CO_2$. Our results indicate that processes other than re-

[5] Unless specifically mentioned the differential reaction rate is defined as volumes (STP) of $H_2+CO$ reacted per volume of catalyst space per hour, as given by $r = dx/d(1/S)$, where $x$ is the fraction of $H_2+CO$ reacted and $S$ is the hourly space velocity expressed as volumes (STP) of $H_2+CO$ fed to the reactor per unit volume of catalyst space per hour. The subscript zero denotes an extrapolated differential reaction rate at $x=0$. In a later part of this section a differential reaction rate in terms of volumes of CO reacted per unit volume of catalyst space per hour is also used.

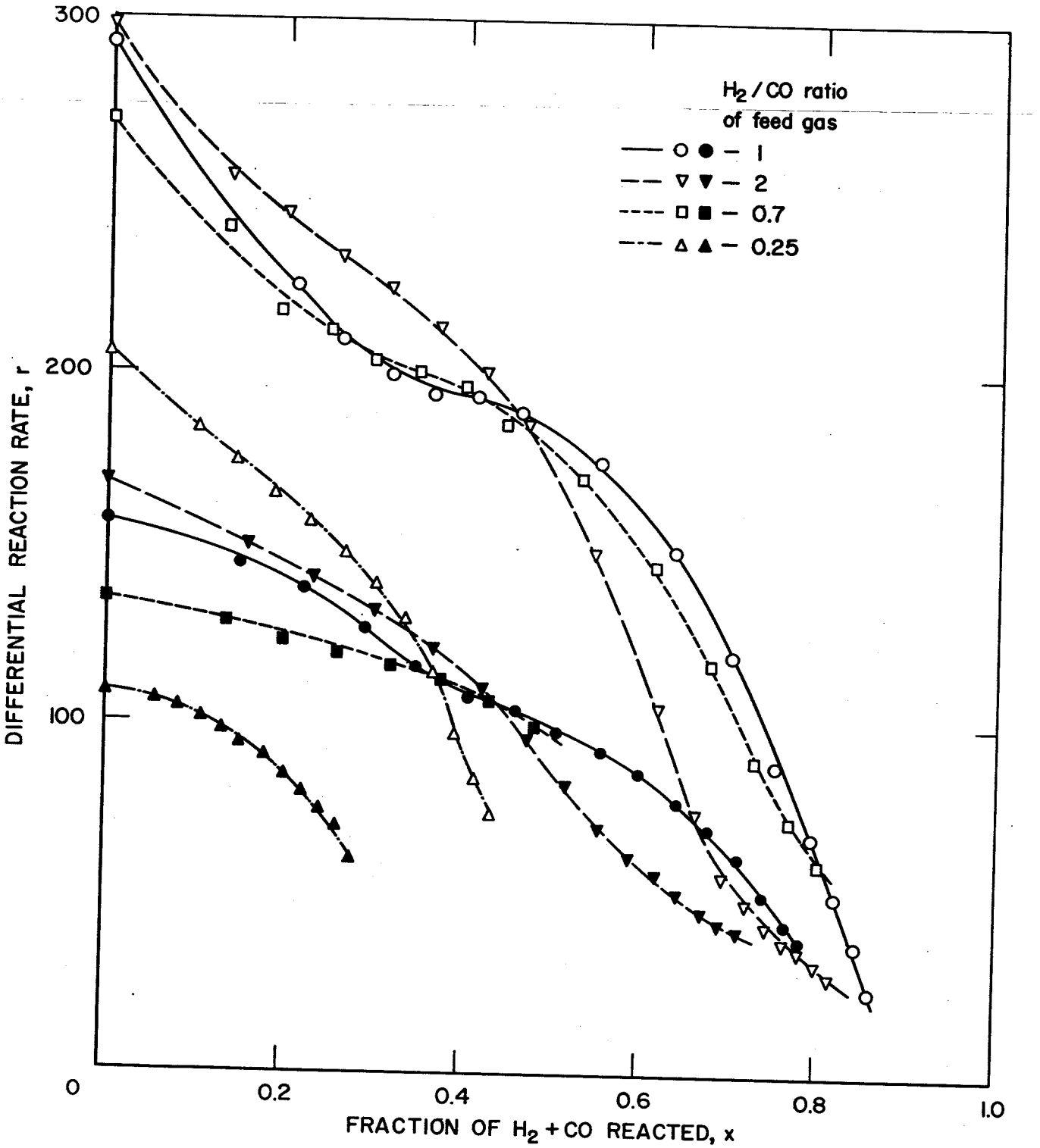


FIGURE 24.—Differential Reaction Rates Obtained by Numerical Differentiation. Open symbols denote 240°C; solid symbols, 225°C.

action (21) must also produce $CO_2$. First, the second term in equation (29) is too small to cause the observed production of $CO_2$. Second, if all $CO_2$ were produced by equation (21), the quantity $r_{CO}/p_{H_2}^{0.6}p_{CO}^{0.4}$ should be constant for a given temperature. The quantity $r_{CO}=$ $dx_{CO}/d(1/S_{CO})$, where $x_{CO}$ is the fractional conversion of CO and $S_{CO}$ the volumes of CO (STP) fed to the reactor per volume of catalyst space per hour, was determined by numerical differentiation. The values of $r_{CO}/p_{H_2}^{0.6}p_{CO}^{0.4}$ were not constant.

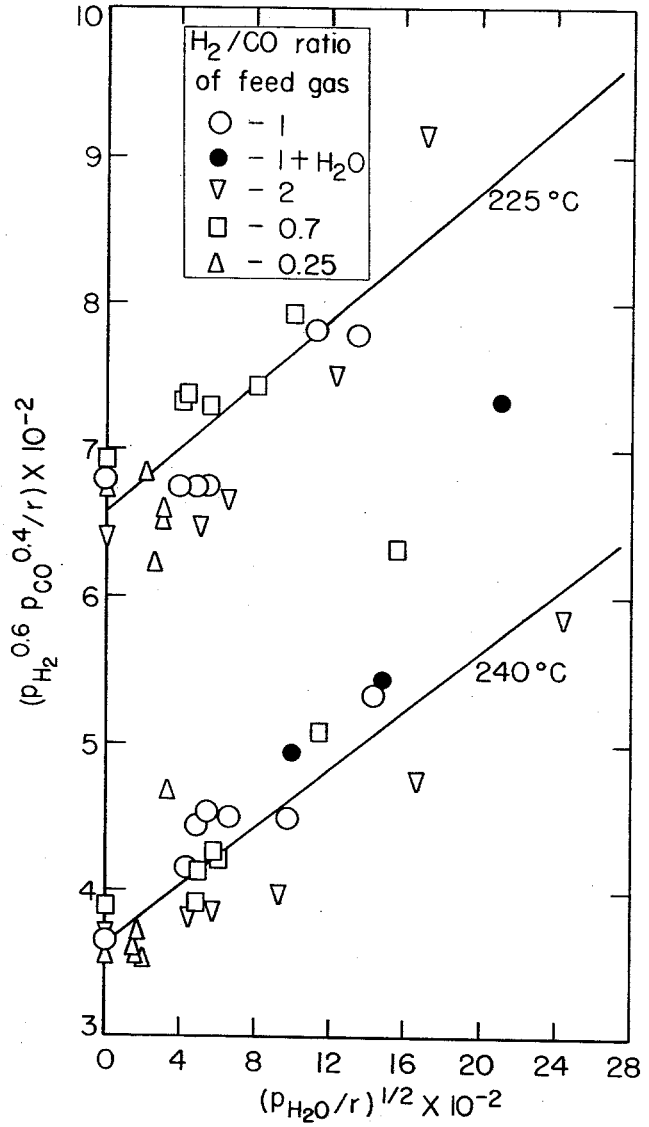


FIGURE 25.—Plots of Equation (29) for Nitrided Fused Iron Catalyst D3001 at 21.4 Atmospheres.

For a given feed gas, $CO_2$ production compared at constant conversions is essentially independent of temperature and pressure. Thus, the processes producing $CO_2$ have about the same dependence on temperature and pressure as the primary synthesis reaction. Kul'kova and Temkin (*43*) presented a rate equation for the water-gas shift on iron oxide catalysts that at least qualitatively described the production of $CO_2$ in the Fischer-Tropsch synthesis in terms of gas composition and had the same dependence on operating pressure (*32*). The activation energy of the principal constant of this equation was 16.5 kcal/mole in the temperature range 400° to 500° C.

In synthesis experiments with iron catalysts in which $C^{14}O_2$ was added to $1H_2+1CO$ feed, Hall, Kokes and Emmett (*26*) reported that $C^{14}$ was not found in sizable quantities in either the carbon monoxide remaining or hydrocarbons produced. This result could arise from the following situations. (1) All the $CO_2$ is produced by a series of steps, of which at least one is irreversible, coupled with the primary synthesis reaction, or (2) the water-gas shift occurs, but the reverse reaction is slow compared with the forward reaction. The present rate equation requires the production of most of the $CO_2$ by processes other than the postulated primary synthesis reactions. For the Kul'kova-Temkin equation with concentrations typical of the synthesis, the rate of the reverse shift is only about 2 percent of the forward reaction. Thus, the reverse shift may be sufficiently slow to explain the results of Hall, Kokes, and Emmett (*26*).

Although the kinetic equation presented here was derived from a simple model based on available concepts of the reaction mechanism, it must be regarded as a semifundamental rate expression for these reasons: (1) Surface coverages are approximated by Freundlich isotherms with the exponents adjusted to provide the observed dependence of rate on gas composition and total pressure; (2) diffusion of reactants and products in oil-filled catalyst pores coupled with the reaction at the surface is important in the present system (*3*, *54*). The assumption is made that the effects of diffusion will change only the values of exponents, but not the nature of the rate equation. For very simple hypothetical reactions this assumption is valid; (3) methane production (as well as reactions producing carbon which are unimportant for the present system) has been ignored. In addition the present equation does not account for the small inhibiting effect of $CO_2$ on rate (*32*).

Blyholder and Emmett (*13*, *14*) investigated the incorporation of tagged ketene in the Fischer-Tropsch synthesis on iron ctalysts. Ketene apparently dissociates to methylene and carbon monoxide on the catalyst. The methylene radical initiates the formation of higher hydrocarbons in the same way as ethanol added to the feed, but the carbon monoxide from ketene acts the same as gaseous carbon monoxide. These results suggest, but do not necessarily prove, that the $C_1$ complex in the synthesis is methylene. The present kinetic scheme can be modified, at least superficially, to accommodate this type of $C_1$ complex. The postulate of methylene as the $C_1$ complex requires an extensive reconsideration of current concepts of the synthesis mechanism, especially the formation of oxygenated molecules.